Protein Crosslinking Improves the Thermal Resistance of Plastocyanin Immobilized on a Modified Gold Electrode

José Luis Olloqui-Sariego[a,*], Antonio Díaz-Quintana[b], Miguel A. De la Rosa [b], Juan José Calvente[a], Inmaculada Márquez[a], Irene Díaz-Moreno[b], Rafael Andreu[a]

[a]Departamento de Química Física

Universidad de Sevilla

Profesor García González, 1

41012, Sevilla (Spain)

[b]Instituto de Investigaciones Químicas, cicCartuja.

Universidad de Sevilla – Consejo Superior de Investigaciones Científicas (CSIC)

Américo Vespucio 49

41092, Sevilla (Spain)

*****Corresponding author

Phone: +34-954557177

E-mail: jlolloqui@us.es (J. L. Olloqui-Sariego)

Abstract

Increasing the thermal stability of immobilized proteins is a motivating goal for improving the performance of electrochemical biodevices. In this work, we propose the immobilization of crosslinked plastocyanin from the thermophilic cyanobacterium *Phormidium laminosum* by simultaneous incubation of a mixture of plastocyanin and the coupling reagents. The thermal stability of the so built covalently immobilized protein films has been assessed by cyclic voltammetry in the 0 - 90ºC temperature range and has been compared to that of physisorbed films. It is shown that the protein loss along a thermal cycle is significantly reduced in the case of the crosslinked films, whose redox properties remain unaltered along a cyclic heating-cooling thermal scan, and can withstand the contact with 70ºC solutions for four hours. Comparison of thermal unfolding curves obtained by circular dichroism spectroscopy of both free and crosslinked protein confirms the improved thermal resistance of the crosslinked plastocyanin. Notably, the electron transfer thermodynamics of physisorbed and crosslinked plastocyanin films are quite similar, suggesting that the formation of intra- and inter-protein amide bonds do not affect the integrity and functionality of the copper redox centers. UV-Vis absorption and circular dichroism measurements corroborate that protein crosslinking does not alter the coordination geometry of the metal center.

Keywords: Thermophilic Plastocyanin; Protein Thermostability; Covalent Crosslinking; Multilayered Protein Film; Temperature Variable Voltammetry.

1. Introduction

The development of integrated biodevices that operate at high temperatures is of great interest for a variety of technological applications [1,2]. Proteins isolated from thermophilic or hyperthermophilic organisms [3,4] are frequently used for this purpose. Satisfactory results are also achievable by site directed mutagenesis [5,6] and chemical immobilization [7-11] procedures. In a previous work, we showed that a physisorbed plastocyanin from the thermophilic cyanobacterium *Phormidium laminosum* (Pho-WT) retains its redox activity at temperatures as high as 90 °C [12]. However, a loss of electroactive proteins occurs at high temperatures, likely due to desorption from the electrode surface, thereby averting their potential use in technological applications. In order to circumvent this drawback and simultaneously improve the thermal stability of the immobilized plastocyanins, we have tested a covalent immobilization protocol based on the simultaneous incubation and deposition of a mixture of Pho-WT and the crossing coupling reagents 1-ethyl-3-(3-dimethylaminopropyl) carbodiimide (EDC) and N-hydroxysulfosuccinimide (NHS) on a cysteamine modified gold electrode. This immobilization protocol, which is expected to cause an extensive intra- and inter-protein coupling [13], results in the formation of a crosslinked multilayered protein assembly. In this report, we assess the kinetics and thermodynamics of the electron exchange between this protein film and the electrode by recording its voltammetric response in the 0º- 90ºC temperature range, and we compare these results with those obtained from a physisorbed protein film. The electron transfer characteristics of both films turned out to be quite similar, indicating that the formation of intra- and inter-protein amide bonds has only a mild influence on the redox activity of the copper active center. However, the thermal stability improved substantially in the case of the crosslinked plastocyanin film

as it will be shown below. UV-Vis and circular dichroism measurements of free and crosslinked plastocyanin at variable temperature support these findings.

2. Materials and methods

Recombinant forms of wild type plastocyanin from *Phormidium laminosum* were expressed in *E.Coli* and purified as described previously [14]. Cysteamine, 1-Ethyl-3-(3-dimethylaminopropyl) carbodiimide (EDC), N-hydroxysulfosuccinimide sodium salt (NHS) and anhydrous dihydrogen sodium phosphate were from Sigma Aldrich, and copper sulphate pentahydrate was from Panreac. All these reagents were used as received. The working electrode was a polycrystalline gold disk with a geometric area of 0.0314 cm^2, and with a surface roughness factor of 1.4 as estimated from the electrical charge associated with the formation and dissolution of a gold oxide layer [15]. Prior to measurements, the gold surface was cleaned by successively polishing with 0.3 and 0.05 μm alumina, rinsed with Millipore water and sonicated. Then it was chemically cleaned using a "*piranha"* solution. Cysteamine self-assembled monolayers were prepared by immersing the gold electrode in a 1mM cysteamine solution in ethanol for 2h at 4°C. Covalent protein immobilization was carried out by exposing the modified electrode surface to a mixture of three droplets: a 4.5 μL drop of 20 mM NHS, a 5.5 μL drop of 40 mM EDC and a 6 μL drop of a 100μM plastocyanin solution for 16 h at room temperature. All these solutions were prepared in 0.01 M sodium phosphate buffer (SPB) at pH 7. Then, the electrode was thoroughly rinsed with water and the working solution. A similar immobilization protocol was applied to physisorb plastocyanin onto the cysteamine modified gold electrode, except for the absence of the NHS and EDC coupling reagents in the solutions of the first two drops indicated above. To physisorb the Cu(II) cation at the cysteamine modified electrode, the modified

electrode was exposed to a 5 μM $CuSO_4$, 0.01 M SPB pH 7 solution for eight hours. Then the electrode was rinsed with water and transferred to the electrochemical cell containing the Cu(II)-free working solution.

Linear scan voltammetric measurements were performed with an AUTOLAB PGSTAT 30 from Eco Chemie B.V, in a three-electrode undivided glass cell, equipped with a gas inlet and thermostated with a water jacket. The counter and reference electrodes were a Pt bar and a Ag/AgCl/NaCl saturated electrode, respectively. The reference electrode was connected to the cell solution via a salt bridge, and kept at room temperature (23 ± 2ºC) in a non-isothermal configuration. Reported potential values have been corrected to the NHE potential scale by adding +192 mV. All measurements were carried out under argon atmosphere. Working solutions contained 0.1 M sodium phosphate buffer (SPB) at pH 7.0. Positive feedback for ohmic drop compensation was applied for voltammograms recorded at scan rates higher than 1 V s^{-1}.

UV-Vis absorption spectra were obtained at room temperature with an Agilent 8453 spectrophotometer. Plastocyanin concentration was 50μM, and the coupling reagents' concentrations were adjusted to keep the same ratio with the protein concentration than in the deposition solution in a 0.1 M phosphate buffer solution pH 7. The cuvette optical path length was 1 cm.

Circular dichroism spectra were recorded at variable temperature with a Jasco J-815 spectropolarimeter in the 300-900 nm wavelength range. Samples contained 500 μM protein and the coupling reagents' concentrations were adjusted to keep the same ratio with the protein concentration than in the deposition solution in a 0.1 M phosphate buffer solution pH 7. The cuvette optical path length was 0.1 cm.

3. Results and discussion

3.1. Voltammetric Response of Plastocyanin Films

Figure 1 compares some typical voltammograms of crosslinked (left) and physisorbed (right) plastocyanin films, recorded at low (v = 0.002 V s^{-1}), intermediate (v = 0.02 V s^{-1}) and high (v = 10 V s^{-1}) potential scan rates. Both films display surface waves, whose faradaic charge Q decreases markedly upon increasing the scan rate.

Irrespective of the immobilization protocol, the surface concentration of electroactive plastocyanins (Γ) calculated from the faradaic charge as: $\Gamma = Q / F \cdot A$, where F is Faraday's constant and A the electrode surface area, remains constant at very low scan rates, it then decreases upon increasing the scan rate, until it reaches a high scan rate limit of $\Gamma \sim 12$ pmol cm^{-2} for $v \geq 10$ V s^{-1} (Figure 2a). Given that plastocyanin can be modeled as a cylinder of 3 nm diameter and 4 nm height [16], a compact protein monolayer would amount to ~14 pmol cm^{-2} for a microscopically flat surface, or to ~20 pmol cm^{-2} for our slightly roughened gold electrode, so that the amount of protein that is being sampled at high scan rates corresponds approximately to the first protein monolayer contacting the electrode surface. Accordingly, one can infer that only ~ 60% of the total plastocyanin immobilized in the first monolayer is electroactive. On the other hand, the total Γ values estimated from the low scan rate limit correspond to fourteen and eleven layers of crosslinked (left) and physisorbed (right) plastocyanin films, respectively, indicating that crosslinking plastocyanin accumulates more protein in the film. A similar voltammetric response has been reported by Lisdat et al. [17,18] for cytochrome c multilayers immobilized on gold electrodes, and it is consistent with the theoretical predictions of Laviron et al. [19] and Calvo et al. [20] for charge transport in space distributed redox modified electrodes.

The formal standard potential ($E_{1/2}$) of the immobilized proteins can be estimated from the average of the anodic and cathodic peak potentials. As can be seen in Figure 2b, $E_{1/2}$ becomes systematically more positive (by ~40 mV) upon increasing the scan rate. Since in the multilayer scenario $E_{1/2}$ values correspond either to the overall formal potential of the protein film at low scan rates, or to the formal potential of the first protein layer at high scan rates, the experimental variation of $E_{1/2}$ with scan rate likely reflects differences in the local protein environment across the multilayer film.

Information on the electron transfer kinetics can be obtained from the dependence of voltammetric peak potential separation (ΔE_p) on the potential scan rate (see figure 2c). The observed non-zero value of ΔE_p indicates that the protein redox conversion is kinetically controlled along the whole potential scan rate interval. However, a comparison of the experimental data with the theoretical prediction of the Butler-Volmer formalism reveals that only at high scan rates the redox conversion approaches the linear ΔE_p vs. ln v behavior expected for a kinetically-controlled electron transfer of a homogeneous redox monolayer. The non-ideal dependence of ΔE_p on the scan rate at low scan rates agrees with the expected behavior for charge transport in multilayered film [19, 20]. According to this view, several protein layers contribute to the observed current at low potential scan rates, where the voltammetric peak separation ΔE_p is controlled by the rate of charge propagation across the protein film. On the other hand, only the first protein layer, close to the electrode surface, contributes to the observed current at high scan rates, and ΔE_p is interpreted then as a measure of the electron transfer rate of this first protein layer. Note that, at high scan rate, the peak separation is greater for the crosslinked plastocyanin, indicating a slower electron transfer rate. This effect could be ascribed to a lower flexibility of the

covalently bound proteins [21], that results in a less effective orientation for electron exchange with the electrode.

Based on these results, it can be concluded that the two immobilization protocols considered here lead to the formation of multilayer assemblies with similar voltammetric responses at low temperatures.

3.2. Influence of Temperature on the Voltammetry of Plastocyanin Films

To assess the impact of the immobilization protocol on the thermal stability of the protein films, gold electrodes modified with either physisorbed or crosslinked proteins were subjected to a thermal cycle. During this cycle, that lasted ~ 6 h, the temperature was first increased from 0 ºC to 90 ºC in steps of 10ºC, and then lowered to 0 ºC in an analogous way. At each thermal step, voltammograms were recorded for thirteen potential scan rates in the 0.02 - 200 V s^{-1} range. Figure 3a illustrates how the amount of electroactive plastocyanin varies along a thermal cycle for the crosslinked (left) and physisorbed (right) protein films. For the physisorbed film, a continuous protein loss up to ~ 80% of the initial population is observed along the thermal cycle, as reported previously for plastocyanin physisorbed on graphite [12], but only a ~ 25% of the initial electroactive protein population is lost for the crosslinked film. Notably, the overall formal potentials (i. e. $E_{1/2}$ determined al low scan rates) of the crosslinked film are the same in the forward and backward thermal scans, whereas they differ significantly in the case of the physisorbed film (see Figure 3b). These results suggest that the physisorbed film becomes partially denatured after being exposed to the highest temperatures, while the molecular structure of the crosslinked proteins remain unaltered, showing thus an improved thermal resistance. Nevertheless, it should be noted that the variation of $E_{1/2}$ with temperature of the two films coincides in the forward thermal

scan, showing that initially both protein assemblies display identical redox thermodynamics. The variations of standard entropy (ΔS^0_{rc}) and enthalpy (ΔH^0_{rc}), associated with the reduction of plastocyanin in these films, were estimated from the slopes of the $E_{1/2}$ vs. T and $E_{1/2}/T$ vs. 1/T plots respectively. Their values ΔS^0_{rc} = - 65 ± 4 J mol^{-1} K^{-1} and ΔH^0_{rc} = - 54 ± 3 kJ mol^{-1}, are less negative than those obtained when the protein was adsorbed on either graphite [12] or alkyldithiol monolayers [22], suggesting a tighter protein structure upon adsorption on cysteamine monolayers, that requires a smaller solvent reorganization upon changing the redox state. This finding indicates that the formation of intra- and inter-protein amide bonds in the crosslinked film seems to not affect the integrity and functionality of the copper redox centers. Figure 3c illustrates the variation of the high scan rate peak separation ΔE_p along the thermal scan, which is a measure of the electron transfer rate of the first protein monolayer. It may be observed that the ΔE_p values of the crosslinked film remain the same in the forward and reverse thermal scans, while the ΔE_p values obtained from the physisorbed film become significantly lower in the reverse thermal scan, stressing again the improved thermal stability of the crosslinked film.

The impact of protein crosslinking on conformational changes in the vicinity of the metal center has been assessed by UV-vis absorption and circular dichroism measurements (Figure 4). We have recorded absorption spectra of the mixture of oxidized plastocyanin and crosslinking reagents for 16 hours after mixing. The spectrum is characterized by an intense S(Cys)→Cu-(II) ligand to metal charge transfer absorption band, at approximately 600 nm, and a much weaker band at 450 nm. It can be observed that these absorption features barely change with time after mixing. We have also recorded the circular dichroism (CD) spectra of both free and crosslinked

oxidized plastocyanin, and can be seen to be nearly superimposable, showing that the crosslinked plastocyanin retains the basic geometry of the metal center. Finally, we have compared the fluorescence spectrum of free and crosslinked proteins. The fluorescence of tryptophan and tyrosine residues are sensitive to their electronic environment, and the increase in quantum yield suggests that these residues become buried in a more compact environment after plastocyanins have reacted with the coupling reagents.

The thermal resistance of the crosslinked protein film was tested also by monitoring its voltammetric response while the electrode was continuously exposed to a working solution at 70ºC, which is a temperature close to the plastocyanin melting point in solution [26]. Data in Figures 4a and 4b show that the midpoint potentials $E_{1/2}$ and the anodic peak current i_p^a remain unchanged during the first four hours of exposure to the hot solution. Then, both voltammetric features start to display a systematic variation with time, pointing to the development of structural changes in the film that affect the energetics of the redox centers. In fact, the observed voltammetric changes are to be expected when thermal denaturation releases the copper ions from the protein matrix. Free copper ions are reduced to Cu(0), rather than to Cu(I) as in plastocyanin, which can dissolve and accumulate in the underlying gold substrate, shifting the formal potential and producing the asymmetrical voltammetric shapes typical of anodic stripping processes [27]. Figure 3c illustrates how the voltammetric response of immobilized plastocyanin evolves, for long exposure times to the hot solution, towards that obtained from free copper cations physisorbed on a cysteamine modified gold electrode.

To corroborate the improved thermal stability of the crosslinked protein in relation to the free one, we have displayed in Figure 6 their normalized unfolding curves in the 20º-100ºC temperature range, as derived from their CD spectra. The normalized curves were fitted to a simple two-state model to estimate their melting points (T_m) [28], and T_m

values of $74.1 \pm 0.3^{o}C$ and $78.5 \pm 0.3^{o}C$ were estimated for free and crosslinked plastocyanins, respectively, corroborating the increase of thermal resistance upon crosslinking that was derived from the voltammetric results.

4. Conclusions

We have shown how the formation of crosslinked protein films substantially increases the thermal stability of immobilized plastocyanin. This crosslinked films are easily prepared in one step by incubating simultaneously the protein and the cross-coupling reagents on the surface of a chemically modified electrode. Interestingly, the crosslinked films display redox properties similar to those observed for physisorbed films, indicating that the formation of intra- and inter-protein amide bonds does not affect the integrity and functionality of the copper redox centers. The immobilization protocol herein described can be considered as a step towards the development of bioelectrochemical devices operating at high temperatures.

Acknowledgments

Authors gratefully acknowledge the technical support by Dr. Estrella Frutos.

J. L. O., I. M., J. J. C. and R. A. acknowledge financial support from the Spanish Ministry of Economy and Competitiveness and the European Union FEDER (grants CTQ2014-52641-P and CTQ2015-71955-REDT (ELECTROBIONET)) and I. D. M., M. A. R. and A. D. Q. acknowledge support from the Spanish Ministry of Economy, Industry and Competitiveness (BFU2015-71017/BMC), Ramón Areces Foundation (2015-2017) and the Andalusian Government (BIO198).

References

[1] M. Lehmann, L. Pasamontes, S.F. Lassen, M. Wyss, The Consensus Concept for Thermostability Engineering of Proteins. Biochim. Biophys. Acta 1543 (2000) 408-415.

[2] H. Yu, H. Huang, Engineering Proteins for Thermostability through Rigidifying flexible sites. Biotech. Adv. 32 (2014) 308–315.

[3] G. D. Haki, S. K. Rakshit, Developments in Industrially Important Thermostable Enzymes: A Review. Biores. Tech. 89 (2003) 17–34.

[4] S. Elleuche, C. Schäfers, S. Blank, C. Schröder, G. Antranikian, Exploration of Extremophiles for High Temperature Biotechnological Processes. Cur. Op. Microbiol. 25 (2015) 113–119.

[5] K. Hernandez, R. Fernandez-Lafuente, Control of protein immobilization: Coupling immobilization and site-directed mutagenesis to improve biocatalyst or biosensor performance, Enz. Microb. Tech. 48 (2011) 107–122.

[6] H. J Wijma, R. J. Floor, D. B Janssen, Structure- and sequence-analysis inspired engineering of proteins for enhanced thermostability, Cur. Op. Struct. Biol. 23 (2013) 588–594.

[7] C. Mateo, J. M. Palomo, G. Fernandez-Lorente, J. M. Guisán, R. Fernandez-Lafuente, Improvement Of Enzyme Activity, Stability And Selectivity Via Immobilization Techniques. Enz. Microb. Tech. 40 (2007) 1451–1463.

[8] K. M Polizzi1, A. S Bommarius, J. M Broering, J. F. Chaparro-Riggers. Stability Of Biocatalysts. Cur. Op. Chem. Biol. 11 (2007) 220–225.

[9] R. A. Sheldon, Cross-Linked Enzyme Aggregates (CLEAs): Stable and Recyclable Biocatalysts, Biochem Soc. Trans. 35 (2007) 1583-1587.

[10] D. Brady, Advances in Enzyme Immobilisation, Biotechnol. Lett. 31 (2009) 1639-1650.

[11] J. D. Cui, S. R. Jia, Optimization Protocols and Improved Strategies of Cross-linked Enzyme Aggregates Technology: Current Development and Future Challenges, Crit. Rev. Biotechnol. 35 (2015)15-28.

[12] J. L. Olloqui-Sariego, E. Frutos-Beltrán, E. Roldán, M. A. De la Rosa, J. J. Calvente, A. Díaz-Quintana, R. Andreu, Voltammetric study of the adsorbed thermophilic plastocyanin from Phormidium laminosum up to 90 °C, Electrochem. Commun. 19 (2012) 105-107.

[13] J. L Olloqui-Sariego, G. S. Zakharova, A. A. Poloznikov, J. J. Calvente, D. M. Hushpulian, L. Gorton, R. Andreu, Interprotein Coupling Enhances the Electrocatalytic Efficiency of Tobacco Peroxidase Immobilized at a Graphite Electrode, Anal. Chem. 87 (2015) 10807-10814.

[14] M. J. Feio, A. Díaz-Quintana, J. A. Navarro, M. A. De la Rosa, Thermal Unfolding of Plastocyanin from the Mesophilic Cyanobacterium *Synechocystis* sp. PCC 6803 and Comparison with Its Thermophilic Counterpart from *Phormidium laminosum*, Biochemistry 45 (2006) 4900-4906.

[15] U. Oesch, J. Janata, Electrochemical Study of Gold Electrodes with Anodic Oxide Films-I. Formation and Reduction Behaviour of Anodic Oxides on Gold, Electrochim. Acta. 28 (1983) 1237–1246.

[16] A. G. Sykes, Plastocyanin and the Blue Copper Proteins, Structure and Bonding 75 (1991) 175-224.

[17] E. Laviron, L. Roullier, C. Degrand, A Multilayer Model for the Study of Space Distributed Redox Modified Electrodes. Part II. Theory and Application of Linear Potential Sweep Voltammetry for a Simple Reaction, J. Electroanal. Chem. 112 (1980) 11–23.

[18] M. Tagliazucchi, E. J. Calvo, Charge Transport in Redox Polyelectrolyte Multilayer Films: The Dramatic Effects of Outmost Layer and Solution Ionic Strength, ChemPhysChem 11 (2010) 2957–2968.

[19] M. K. Beissenhirtz, F. W. Scheller, F. Lisdat, A Superoxide Sensor Based on a Multilayer Cytochrome c Electrode, Anal. Chem. 76 (2004) 4665–4671.

[20] D. Sarauli, J. Tanne, D. Schäfer, I. W. Schubart, F. Lisdat, Multilayer Electrodes: Fully Electroactive Cyt c on Gold as part of a DNA/Protein Architecture, Electrochem. Commun. 11 (2009) 2288–2291.

[21] H. B. Gray, J. R. Winkler, Electron tunneling through proteins, Q. Rev. Biophys. 36 (2003) 341–372.

[22] J. L. Olloqui-Sariego, B. Moreno-Beltrán, A. Díaz-Quintana, M. A. De la Rosa, J. J. Calvente, R, Andreu, Temperature Driven Changeover in the Electron Transfer Mechanism of a Thermophilic Plastocyanin, J. Phys. Chem. Lett. 5 (2014) 910–914.

[23] E. I. Solomon, R. K. Szilagyi, S. De Beer George, L. Basumallick Electronic Structures of Metal Sites in Proteins and Models: Contributions to Function in Blue Copper Proteins, Chem. Rev. 104 (2004) 419-458.

[24] L. B. LaCroix, D. W. Randall, A. M. Nersissian, C. W. G. Hoitink, G. W. Canters, J. S. Valentine, E. I. Solomon, Spectroscopic and Geometric Variations in Perturbed Blue Copper Centers: Electronic Structures of Stellacyanin and Cucumber Basic Protein, J. Am. Chem. Soc. 120 (1998) 9621-9631.

[25] L. B. LaCroix, S. E. Shadle, Y. Wang, B. A. Averill, B. Hedman, K. O. Hodgson, E. I. Solomon, Electronic Structure of the Perturbed Blue Copper Site in Nitrite Reductase: Spectroscopic Properties, Bonding, and Implications for the Entatic/Rack State, J. Am. Chem. Soc. 118 (1996) 7755-7768.

[26] F. J. Muñoz-López, E. Frutos-Beltrán, S. Díaz-Moreno, I. Díaz-Moreno, G. Subías, M. A. De la Rosa, A. Díaz-Quintana, Modulation of copper site properties by remote residues determines the stability of plastocyanins. FEBS Lett. 584 (2010) 2346–2350.

[27] J. J. Calvente, R. Andreu, Accurate Analytical Expressions for Stripping Voltammetry in the Henry Adsorption Limit, Anal. Chem. 83 (2011) 6401–6409.

[28] J. Sancho, The stability of 2-state, 3-state and more-state proteins from simple spectroscopic techniques... plus the structure of the equilibrium intermediates at the same time. Arch. Biochem. Biophys. 531 (2013) 4-13.

Figure captions

Figure 1.- Cyclic voltammograms of Pho-WT immobilized at a cysteamine-modified gold electrode by covalent crosslinking (left panels) or physisorption (right panels) recorded in 0.1M sodium phosphate buffer solution of pH 7 at 0ºC and the indicated potential scan rates.

Figure 2.- (a) Surface concentration, (b) midpoint redox potential and (c) peak potential separation of electroactive plastocyanin as a function of the potential scan rate. Plastocyanin was immobilized at a cysteamine-modified gold electrode by either covalent crosslinking (left panels) or physisorption (right panels). Dashed lines in (a) mark the theoretical estimate for a protein monolayer. Solid lines in (c) are theoretical fits computed from the Butler-Volmer formalism with k_S^{app} values of ~15 s^{-1} and ~25 s^{-1} for crosslinked and physisorbed films, respectively. Voltammograms were recorded in a 0.1M sodium phosphate buffer solution of pH 7 at 0ºC.

Figure 3.- (a) Electroactive surface concentration, (b) midpoint redox potential and (c) peak potential separation as a function of temperature along a thermal cycle, corresponding to Pho-WT immobilized by either covalent crosslinking (left panels) or physisorption (right panels) at a cysteamine-modified gold electrode. Dark symbols were obtained during the forward heating scan and light symbols during the reverse cooling scan. Γ and $E_{1/2}$ values were determined at 0.02 V s^{-1}, and ΔE_p values were obtained at 50 V s^{-1}.

Figure 4.- (a) UV-Vis absorption spectrum of oxidized Pho and of its mixture with the crosslinking reagents, as a function of elapsed time from mixing. Pho concentration is 50 µM. (b) CD spectra and (c) Fluorescence spactra of free (red line) and crosslinked (blue line) oxidized Pho. Pho concentration is 500 µM. Other experimental conditions: 0.01 M sodium phosphate buffer, pH 7 and 25ºC.

Figure 5.- (a) Midpoint redox potential and (b) anodic peak current corresponding to a crosslinked Pho-WT film as a function of the exposure time to a 70ºC working solution. Dashed lines are just eye guides. (c) Voltammograms recorded for the crosslinked protein film after 0 min (dark blue) and 420 min (light blue) exposure to the 70ºC solution, and voltammogram corresponding to free copper cations physisorbed on a cysteamine-modified gold electrode (green). Potential scan rate is 0.02 V s^{-1}.

Figure 6.- Normalized thermal unfolding curves obtained by circular dichroism spectroscopy of oxidized free (red circles) and crosslinked (blue circles) plastocyanin. Plastocyanin concentration is 500 μM. Other experimental conditions: 0.01 M sodium phosphate buffer, pH 7. Lines are fits using a two state equilibrium model.

FIGURE 1

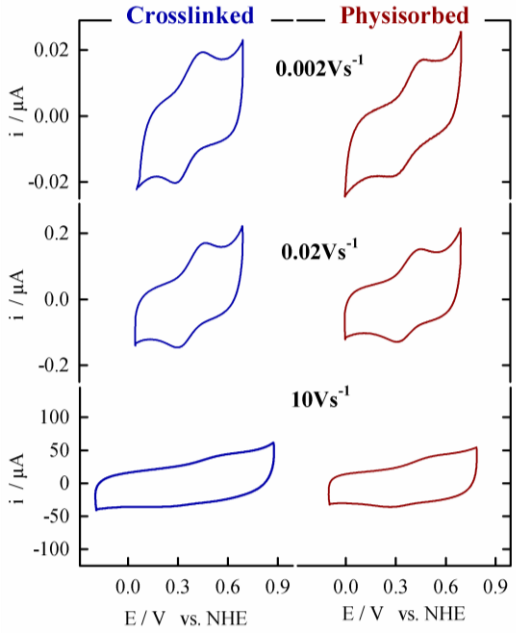
Crosslinked
Physisorbed
0.002Vs-1
0.02Vs-1
10Vs-1
i / µA
0.02
0.00
-0.02
0.2
0.0
-0.2
100
50
0
-50
-100
0.0 0.3 0.6 0.9
E / V vs. NHE

FIGURE 2

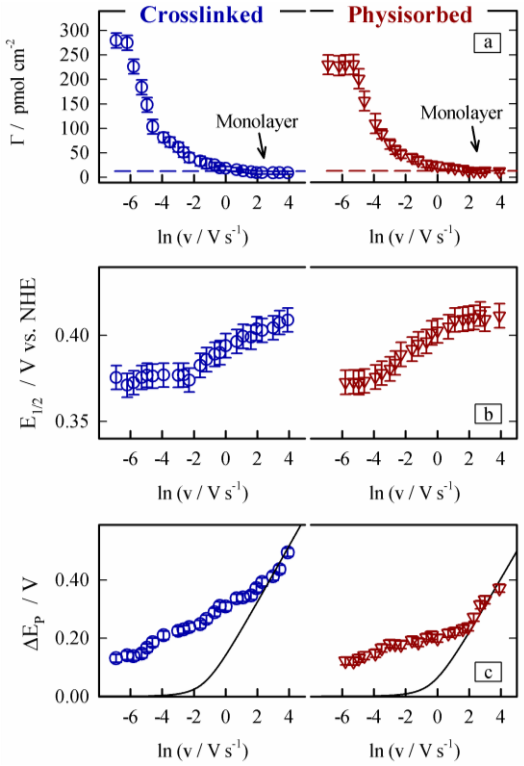
Crosslinked
Physisorbed
a
Monolayer
Monolayer
Γ / pmol cm-2
300
250
200
150
100
50
0
-6 -4 -2 0 2 4
ln (v / V s-1)
b
E1/2 / V vs. NHE
0.40
0.35
c
ΔEP / V
0.40
0.20
0.00

FIGURE 3

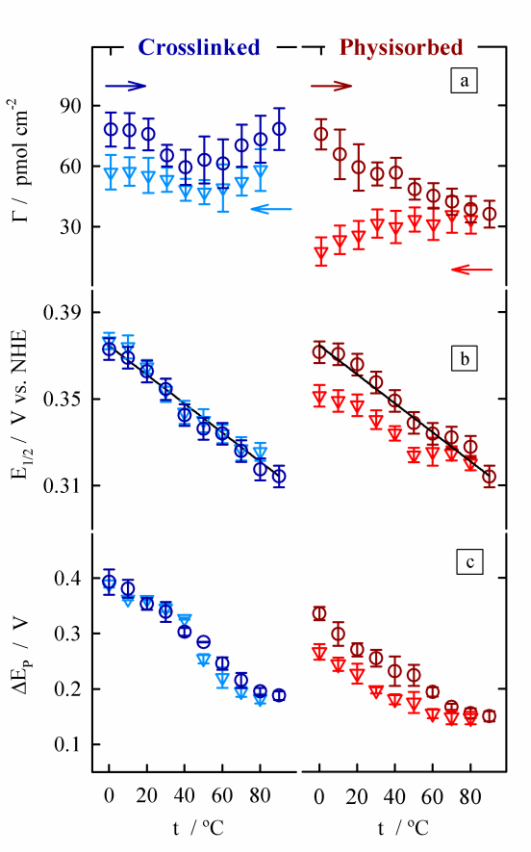
Crosslinked
Physisorbed
a
b
c
Γ / pmol cm-2
E1/2 / V vs. NHE
ΔEp / V
t / °C
t / °C

FIGURE 4

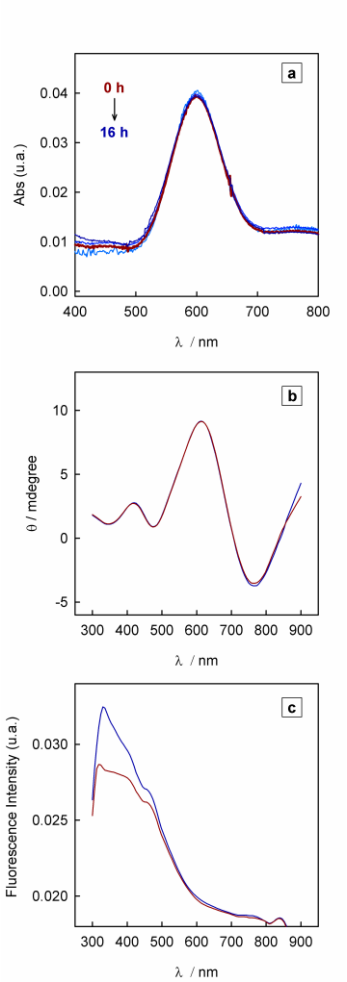
a
0 h
16 h
Abs (u.a.)
0.04
0.03
0.02
0.01
0.00
400
500
600
700
800
λ / nm
b
θ / mdegree
10
5
0
-5
300
400
500
600
700
800
900
λ / nm
c
Fluorescence Intensity (u.a.)
0.030
0.025
0.020
300
400
500
600
700
800
900
λ / nm

FIGURE 5

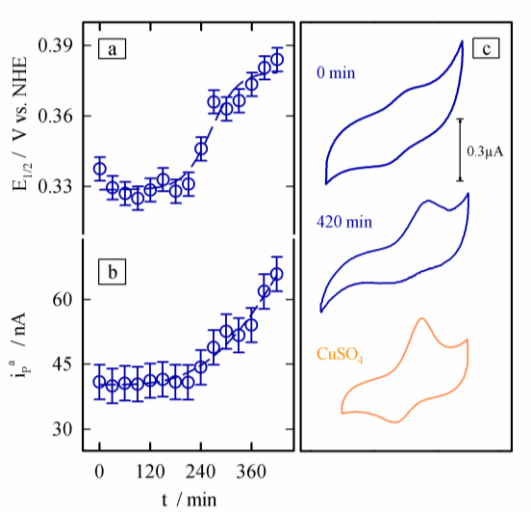
a
b
c
0.39
0.36
0.33
$E_{1/2}$ / V vs. NHE
60
45
30
i_p^a / nA
0
120
240
360
t / min
0 min
420 min
$CuSO_4$
0.3μA

FIGURE 6

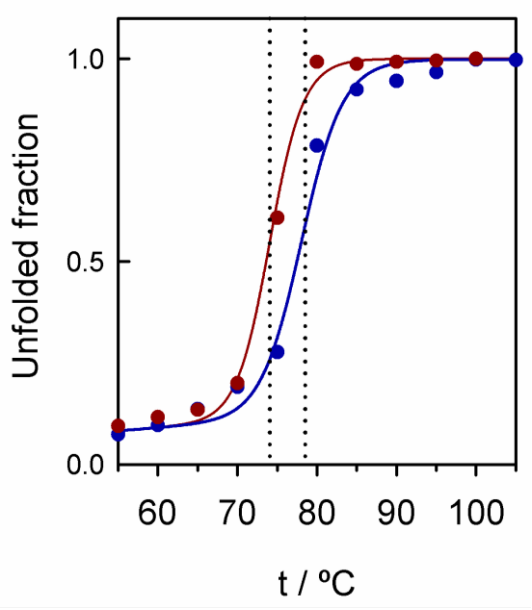

GRAPHICAL ABSTRACT